CONSTRAINING THE PRESSURE THRESHOLD OF IMPACT INDUCED CALCITE TWINNING. P. Lindgren[1], M. C. Price[2], M. R. Lee[1] and M. J. Burchell[2], [1]School of Geographical and Earth Sciences, University of Glasgow, Glasgow G12 8QQ, U.K. email: paula.lindgren@glasgow.ac.uk [2]School of Physical Sciences, University of Kent, Canterbury CT2 7NH, U.K.

Introduction: Calcite twinning is an intra-crystalline microstructure that forms along specific crystallographic planes (e-, r- and f-planes), due to deformation via uniaxial stress (shear stress) [1]. This process is instantaneous and permanently alters the orientation of the crystal. In a twinned calcite grain, there is a geometric relationship between the twin plane, the c-axes and the principal axes of stress (maximum compression and maximum extension) and this relationship is widely applied to infer stress orientations [2]. The calcite twin microstructure can also be used as a tool to determine the stress magnitude, via e.g. twin morphologies, twin thickness and twin densities [3]. However, the critical resolved shear stress necessary to generate calcite twins in the first place is poorly constrained. Generally, a value of 10 MPa is quoted in the literature [4], but this value is dependent on various factors such as the grain size, porosity and strain rate [3,5]. Calcite twins can be used to study the deformation history of terrestrial rocks, but also of calcite-bearing meteorites whose deformation histories are hard to assess owing to their lack of olivine and pyroxene, which are normally used for determining shock-histories of meteorites [6]. Calcite twinning in carbonaceous chondrite meteorites is thought to have formed via impact gardening on the asteroidal parent bodies [7,8]. In terrestrial settings, calcite is usually deformed in tectonic regimes with relatively low strain rates, compared to the higher strain rates that are activated during impacts.

In this study, we have carried out a set of experiments to better constrain the pressure threshold for impact induced calcite twinning. This information is useful for our understanding of carbonaceous chondrite parent bodies, where calcite twins are valuable tools for reconstructing their deformation history [8].

Methods: Four calcite targets were impacted at different conditions using a light-gas gun [9] (Table 1). Calcite speleothems were chosen as targets since these are composed of pure calcite and tectonically undeformed. The resulting craters were analyzed in plan view and in cross section with scanning electron microscopy (SEM) (2D and 3D imaging) and electron backscatter diffraction (EBSD) analyses to determine the depth of twinning. Hydrocode modelling simulating the impact conditions and target properties was carried out using Ansys' AUTODYN-2D (v12.0.1) to determine the pressures and temperatures at different depths in the calcite targets during the cratering process.

Results and discussion: The impact conditions and the properties of the resulting craters in the four targets (A, B, C and D) are presented in Table 1. All the craters have a zone of severe brecciation and fragmented calcite grains occurring just below the crater floor. The severe brecciation ranges into a zone of intense fracturing and eventually into just minor fractures and apparently unaffected target calcite. The fractures often occur along the calcite cleavage planes.

Table 1. Summary of impact conditions and crater characteristics.

Target sample	A	B	C	D
Target grain size	Coarse ~1 mm	Coarse ~1 mm	Coarse ~1mm	Fine ~60 μm
Projectile diameter and material	0.8 mm (stainless steel)	1.5 mm (glass)	0.8 mm (stainless steel)	0.8 mm (stainless steel)
Impact velocity (km s^{-1})	1.153	1.19	2.03	1.23
Crater diameter (mm)	5.2-6.5	5.3-6.9	7-9.5	3.3-5.8
Crater depth (mm)	2.2	1.7	> 2	2

Crater A has a slightly irregular circumference with only minor fractures surrounding the rim in plan view. Melting is evident in the center of the crater. A cross section of this crater reveals that the projectile is preserved in the target and occurs in a pit below the main excavated crater (Fig. 1a). The depth of intense brecciation below the crater floor is 0.45 mm and the full depth of fracturing below the crater floor is 1.8 mm. Crater B is more regular and bowl-shaped, with radial fractures extending from the rim in plan view. In cross section it contains Si-rich veins penetrating through the crater floor, which must be derived from melting of the glass projectile (Fig. 1b). Crater C formed during higher velocities than the other craters in our experiment, and here a large deep fracture has formed along one side of the crater. There are also some smaller fractures branching out from the opposite side of the crater. Here, melting has been widespread, both at the base of the crater and on the flanks of the large fracture (Fig. 1c). Crater D formed in a finer grained target, with a grain size of ~60 μm rather than ~1 mm. It has an irregular circumference with large

curved fractures extending out from the edge of the crater rim. Similar to crater A, it also has a small pit protruding below the main crater floor.
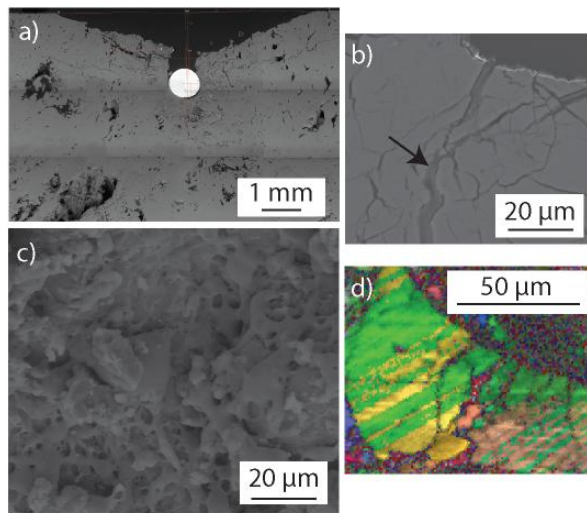

Fig. 1a) SEM-BSE micrograph of a cross section through crater A. Note the preserved steel projectile (white) in the pit protruding below the floor of the main crater. **b)** SEM-BSE micrograph of Si-rich veins (arrow) of melted glass projectile penetrating through the floor of crater B. **c)** SEM-BSE micrograph showing melted calcite at the base of crater C. **d)** EBSD orientation map (IPF colors) of calcite e-twins (green lamellae) from crater A.

Calcite twinning occurs in all the craters, and ongoing work will constrain the depths of twinning using EBSD analyses. The twins occur on the $\{\bar{1}018\}$ planes and hence are calcite e-twins (Fig. 1d). The depth of twinning below the crater A floor is 1.1 mm and the crater depth is 2.2 mm. This gives a total depth of twinning below the target surface of 3.3 mm. Output from the hydrocode simulation for a zero porosity calcite target with an equation of state (EoS) from [10] and a Von Mises strength (yield strength = 410 MPa [11]) are shown in Fig. 2. Contours are of maximum pressure, and a depth of 1.1 mm below the crater floor corresponds to a maximum pressure of ~100 MPa. This value is a factor of ten higher than the value of 10 MPa often cited in the literature [5]. This might be because impact deformation gives higher strain rates than tectonic deformation, and the strain rate will influence the threshold pressure at which calcite twins are generated [5]. Forthcoming results from the other three experimental craters will further constrain the pressure threshold of impact induced twinning along with refinement of the EoS and strength model used for calcite in the hydrocode modelling. However, this experiment shows that calcite twins can form at shock pressures of ≥100 MPa, which are more realistic of impact gardening on asteroids than previous impact experiments on calcite that have been done at high pressures of 85 GPa [12].
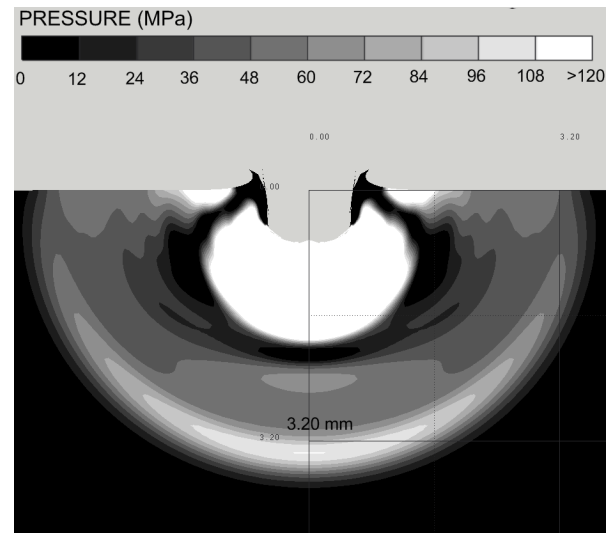

Fig. 2: Output from AUTODYN simulations of 0.8 mm st-st projectile impacting calcite at 1.153 km s^{-1}. Contours are contours of maximum pressure and show a pressure of ~100 MPa was attained at a depth of 3.20 mm below the surface of the target. Note, the impactor has been removed for clarity.

References: [1] De Bresser J.H.P. and Spiers C.J. (1997) *Tectonoph. 272,* 1–23. [2] Turner F.J. (1962) *J. Geophys. Res. 67*, 1660. [3] Burkhard M. (1993) *J. Struc. Geol. 15*, 351-368. [4] Lacombe O. and Laurent P. (1996) *Tectonophys. 255*, 189-202. [5] Lacombe O. (2001) *Tectonics 20*, 834-849. [5] Scott E.R.D. et al. (1992) Geochim. Cosmochim. Acta 56, 4281-4293. [7] Brearley A. et al. (1999) *30th LPSC*, Abstract#1301 [8] Lindgren et al. (2011) *EPSL 306*, 289-298. [9] Burchell M.J. et al. (1999) *Measurem. Sci. Techn. 10*, 41-50. [10] Kalashnikov N. G et al. (1973). *Izv. Akad. Nauk SSSR.,*2,23-29 (via http://teos.ficp.ac.ru/rusbank). [11] Houslow M. J. et al. (2001). *Chem. Eng. Sci. 56,* 2543–2552. [12] Langenhorst et al. (2003) *In:* Davison et al. (editors) High-pressure compression of solids V: Shock chemistry with applications to meteorite impacts. pp. 1-18.